Medical Microbiology and Immunology (2019) 208:651–666
https://doi.org/10.1007/s00430-018-0572-z

ORIGINAL INVESTIGATION

Immune response triggered by *Trypanosoma cruzi* infection strikes adipose tissue homeostasis altering lipid storage, enzyme profile and adipokine expression

Florencia B. González[1] · Silvina R. Villar[1,3] · Judith Toneatto[2] · María F. Pacini[1] · Julia Márquez[1] · Luciano D'Attilio[1] · Oscar A. Bottasso[1] · Graciela Piwien-Pilipuk[2] · Ana R. Pérez[1,3]

Received: 31 July 2018 / Accepted: 30 October 2018 / Published online: 9 November 2018

Abstract

Adipose tissue is a target of *Trypanosoma cruzi* infection being a parasite reservoir during the chronic phase in mice and humans. Previously, we reported that acute *Trypanosoma cruzi* infection in mice is linked to a severe adipose tissue loss, probably triggered by inflammation, as well as by the parasite itself. Here, we evaluated how infection affects adipose tissue homeostasis, considering adipocyte anabolic and catabolic pathways, the immune–endocrine pattern and the possible repercussion upon adipogenesis. During in vivo infection, both lipolytic and lipogenic pathways are profoundly affected, since the expression of lipolytic enzymes and lipogenic enzymes was intensely downregulated. A similar pattern was observed in isolated adipocytes from infected animals and in 3T3-L1 adipocytes infected in vitro with *Trypanosoma cruzi*. Moreover, 3T3-L1 adipocytes exposed to plasmas derived from infected animals also tend to downregulate lipolytic enzyme expression which was less evident regarding lipogenic enzymes. Moreover, in vivo-infected adipose tissue reveals a pro-inflammatory profile, with increased leucocyte infiltration accompanied by TNF and IL-6 overexpression, and adiponectin downregulation. Strikingly, the nuclear factor PPAR-γ is strongly decreased in adipocytes during in vivo infection. Attempts to favor PPAR-γ-mediated actions in the adipose tissue of infected animals using agonists failed, indicating that inflammation or parasite-derived factors are strongly involved in PPAR-γ inhibition. Here, we report that experimental acute *Trypanosoma cruzi* infection disrupts both adipocyte catabolic and anabolic metabolism secondary to PPAR-γ robust downregulation, tipping the balance towards to an adverse status compatible with the adipose tissue atrophy and the acquisition of an inflammatory phenotype.

Keywords *Trypanosoma cruzi* · Chagas disease · PPAR-γ · Adipocytes · Adipose tissue · 3T3-L1

Introduction

Adipose tissue (AT) comprises a variety of cell types, in which mature adipocytes are the predominant cells, although endothelial cells, blood cells, fibroblasts, pericytes, pre-adipocytes and resident macrophages, lymphocytes and regulatory T cells (Tregs) are also included [1]. White adipose tissue (WAT) represents an energy reserve used for periods of wasting or high energy demand. Additionally, the AT is an important endocrine organ with the capacity to produce and release a large number of bioactive molecules involved in the regulation of multiple physiologic and pathologic processes, such as immune defenses and inflammation [2–4]. In particular, WAT participates in the maintenance of the immune response, a process that demands high energy expenditure. Furthermore, it participates in the immune response directly

Edited by: A. Descoteaux.

Electronic supplementary material The online version of this article (https://doi.org/10.1007/s00430-018-0572-z) contains supplementary material, which is available to authorized users.

✉ Florencia B. González
gonzalez@idicer-conicet.gob.ar

[1] Instituto de Inmunología Clínica y Experimental de Rosario (IDICER-CONICET-UNR), Suipacha 590, 2000 Rosario, Argentina

[2] Institute of Biological and Experimental Medicine (IBYME-CONICET), Buenos Aires, Argentina

[3] Centro de Investigación y Producción de Reactivos Biológicos (CIPReB), Facultad de Ciencias Médicas, Universidad Nacional de Rosario, Rosario, Argentina

through mechanisms mediated by resident immune cells such as macrophages, lymphocytes and Tregs and, indirectly, through the systemic release of diverse mediators collectively called adipokines such as leptin, adiponectin, TNF or IL-6, among others [2].

In addition to its secretory function, adipocytes are highly specialized for fat storage and play a fundamental role in tuning energy balance and the overall body homeostasis. The spare energy is deposited in adipocytes in the form of triglycerides through a process denominated lipogenesis. The fatty acids used for triglyceride biosynthesis are mainly taken up from circulation. The enzyme lipoprotein lipase (LPL) plays a critical role in facilitating fatty acids entry into adipocytes by hydrolysis of circulating triglycerides [5]. Once inside the adipocyte, the esterification of fatty acids with glycerol occurs. During the sequential esterification processes acyl-CoA:diacylglycerol acyltransferase (DAGT, isoforms 1 and 2) catalyzes the final and critical step in the triglyceride synthesis pathway playing an important role in adipocyte lipid deposition [6]. Adipocytes also synthesize fatty acid de novo from acetyl-CoA, malonyl-CoA and NADPH by the fatty acid synthase (FAS) [7]. Unlike lipogenesis, lipolysis is the process by which free fatty acids are released from AT after the breakdown of stored triglycerides. The main lipases involved in lipolysis are the adipocyte triglyceride lipase (ATGL) and the hormone-sensitive lipase (HSL) responsible for the conversion of triglycerides to diglycerides and diglycerides to monoglycerides, respectively [8–10].

It is known that adipogenesis, the process of cell differentiation by which pre-adipocytes become mature adipocytes, is highly regulated [11, 12]. The peroxisome proliferator-activated receptor-gamma (PPAR-γ) transcription factor is a dominant regulator of adipogenesis and highly necessary for the maintenance of the mature phenotype [13]. PPAR-γ deletion in mature adipocytes compromises their viability and fat storage because of the expression loss of the main metabolic enzymes of adipocytes [14–16]. On the other hand, PPAR-γ is also expressed in immune cells, leading to the secretion of IL-10 and the inhibition of pro-inflammatory cytokine production [17–21]. In addition, PPAR-γ activation in T lymphocytes may inhibit their expansion and activation by preventing the production of IL-2 [22]. Along with PPAR-γ, the C/EBP transcription factors are also required for a strong adipocyte-specific gene expression [23, 24].

During an infectious process, the host responds with a generalized defence reaction involving changes at the immunological, metabolic and neuroendocrine levels. Acute *T. cruzi* infection in C57BL/6 mice is a well-characterized model in our laboratory from the immunological and endocrine standpoints. These mice course a lethal acute infection, characterized by an exacerbated immune response that triggered the hypothalamus–pituitary–adrenal axis activation with the consequent release of corticosterone into the circulation as a protective response [25, 26]. A possible link between the energetic status and the course of *T. cruzi* infection was raised by the pioneering works of Tanowitz and collaborators [27], documenting that an unfavorable metabolic environment, i.e., diabetes, increased the severity of *T. cruzi* infection. Furthermore, we and other authors have shown that experimental *T. cruzi* infection courses with body weight decrease and severe AT loss [28, 29].

During healthy states, the metabolic status is finely tuned by hormonal signals, the nourishing status and the energy expenditure. The weight loss in acutely *T. cruzi*-infected mice seems to be linked to immune–endocrine disturbances and enhanced energy expenditure. Moreover, AT atrophy might be also directly induced by the parasite, since adipocytes are targets of *T. cruzi* infection. In this regard, many authors propose that AT acts a reservoir of the parasite during chronic infections in mice and humans [29–31].

From the foregoing, in this study we evaluated how acute *T. cruzi* infection affected AT homeostasis; in terms of both anabolic and catabolic pathways, the immune and endocrine response patterns and the possible repercussion on adipogenesis. Here, we report that experimental acute *T. cruzi* infection disrupts both adipocyte catabolic and anabolic metabolism secondary to PPAR-γ robust downregulation, tipping the balance towards an adverse status compatible with the AT atrophy and the clear acquisition of an inflammatory phenotype.

Materials and methods

Mice

Male C57BL/6 mice were bred at the Centro de Investigación y Producción de Reactivos Biológicos (CIPReB) and maintained at the animal facilities of the School of Medicine of Rosario. For some experiments, B6.129S-$^{Tnfrsf1a\ tm1Imx\ Tnfrsf1b\ tm1Imx}$, which lack both types of TNF receptors (TNF-$R_{(1+2)}$KO mice), were used. Animals had free access to food and water, and were handled according to institutional guidelines. 4–6-week-old mice were used throughout the experiments. The study was approved by the Institutional Animal Care and Use Committee of the School of Medicine of National University of Rosario by resolution no. 4977/2013, following the latest National Institute of Health guide for the care and use of laboratory animals.

Parasite strain and maintenance

The Tulahuén strain (DTU VI) [32] of *T. cruzi* used in this study was maintained by serial passages in CBi suckling

mice (from CIPReB). Briefly, suckling mice were infected intraperitoneally with 150,000 trypomastigotes suspended in 100 µl of physiological saline. After 1 week of infection, these mice were anesthetized with xylazine/ketamine (2 mg/kg xylazine + 100 mg/kg ketamine) and euthanized by cardiac puncture. Live blood parasites were counted using a Neubauer's chamber and used to infect other suckling mice.

Experimental infection

For the experiments, blood trypomastigotes of *T. cruzi* were obtained from infected suckling CBi mice. Briefly, the blood was centrifugated at 1500 rpm and the supernatant was separated and centrifugated at 3000 rpm. The pellet was washed twice and resuspended in physiological saline. Parasites were counted using a Neubauer´s chamber. Adult C57BL/6 mice were infected with 1000 trypomastigotes by intraperitoneally route.

Glycemia and lipid profile determination

At different days pi, blood was obtained by cardiac puncture in heparin-containing tubes and the plasmas were separated by centrifugation and stored at − 20 °C. Levels of glucose, triglycerides, cholesterol, LDL and HDL were measured by enzymatic methods (Wiener Lab, Rosario, Argentina).

Adipose tissue histology

After mice were euthanized, the epididymal fat pads were removed, fixed in 10% formaldehyde and embedded in paraffin. Paraffin-embedded 5-µm sections were stained with hematoxylin and eosin. The area of adipocytes and the area occupied by the inflammatory infiltrate (pixel^2) were evaluated by light microscopy and subjected to further digital analysis using the Image J software (Bethesda, Maryland, USA).

Adipocytes and stromal vascular fraction cell isolation by adipose tissue collagenase digestion

To separate mature adipocytes from stromal vascular fraction cells (SVFC), the epididymal AT (EAT) was digested with collagenase type I (Gibco). Briefly, the epididymal fat pads were removed, minced, and digested in 2 ml of Hank's balanced salt solution with 1 mg/ml of collagenase type I and 3 mM of $CaCl_2$, at 37 °C for 2 h. After that time, the solution was filtered by passing through a nylon mesh, to remove the remaining large tissue fragments. The filtered suspension was then centrifuged at 100 rcf for 1 min. After centrifugation, the adipocytes formed a floating layer at the top of the liquid, whereas SVFC deposited at the bottom of the tube. Adipocytes were collected and washed one time with HBSS and then resuspended in TRI Reagent® (Molecular Research Center) for posterior studies by RT-qPCR. SVFC were resuspended in phosphate buffered saline (PBS) supplemented with 3% of fetal bovine serum (FBS; Gibco), for flow cytometry or in TRI Reagent® for RT-qPCR.

Adipose tissue resident immune cell characterization by flow cytometry analysis

For flow cytometry assays, SVFC isolated from infected and control AT were resuspended in PBS/3% FBS and stained in one step with the following surface monoclonal antibodies: FITC-coupled anti-CD4, APC-Cy7-coupled anti-CD8, PE-Cy7 coupled anti-CD11b and FITC-coupled anti-CD11c (all from BD Biosciences). For Foxp3 detection, an intracellular staining was performed using PE-coupled anti-FoxP3 antibody and the corresponding fixation/permeabilization buffers (Mouse regulatory T cell staining kit, eBiosciences). A minimum of 50.000 events was acquired using an ARIAII flow cytometer (Becton-Dickinson, New Jersey, USA). Living cells were gated on the basis of forward- and side-cell scatter. Results were analyzed using DIVA (Becton-Dickinson, New Jersey, USA).

In vivo PPAR-γ agonist treatment

Animals were treated with PPAR-γ agonists 15-deoxy-Δ12,14-prostaglandin J2 (Cayman Chemical Company) and rosiglitazone (Avandia, Glaxo-Smith-Kline). Treatment with PGJ was performed daily between days 7 and 17 post-infection (pi) by intraperitoneal route (dose 1 mg/kg/day). Treatment with RSG was performed daily from day 0 to 17 days pi by intragastric route or "gavage" (dose 20 mg/kg/day). At day 17 pi, mice were sacrificed to obtain blood, EAT and peritoneal macrophages.

Evaluation of mRNA expression of adipose tissue transcription factors, enzymes and adipokines by real-time PCR

Total RNA was isolated from fresh epididymal fat pads, isolated adipocytes or SVFC (immediately after collagenase digestion) or in vitro-cultured 3T3-L1 adipocytes. RNA was isolated using TRI Reagent® and reverse-transcribed to cDNA using the RevertAid Reverse Transcriptase (Thermo Fisher Scientific). Real-time PCR was performed with the StepOnePlus Real-Time PCR System (Applied Biosystems) using a Mix (5x HOT FIREPol® EvaGreen® qPCR Mix Plus (ROX); Solis BioDyne) according to the manufacturer's instructions. The amplification program included an initial activation step at 95 °C for 15 min, followed by denaturation at 95 °C for 15 s, annealing between 60 and 65 °C and finally elongation at 72 °C for 20 s, for 40 cycles. Fluorescence was

measured after each extension step, and the specificity of amplification was evaluated by melting curve analysis. The house-keeping gene RPL13 was used as control to normalize RNA samples. The relative gene expression levels were calculated using a standard curve for each gene. The amplification efficiencies were identical or similar between genes of interest and controls. All primers (Online Resource 1) and probes were designed in our laboratory and purchased from Eurofins Genomics.

3T3-L1 cell culture

3T3-L1 cells were cultured in Dulbecco's Modified Eagle Medium (DMEM) containing 10% (v/v) FBS and 1% (v/v) of penicillin–streptomycin–glutamine (100X; Gibco). First, 200.000 cells/ml were seeded in 60-mm culture dishes with a coverslip in them and propagated as fibroblasts at 37 °C under 5% CO_2 atmosphere. The medium was changed every 2 days until confluence. Confluent cells were induced to differentiate into adipocytes with differentiation medium, as previously described [33]. Briefly, 3T3-L1 cells were grown in DMEM in the presence of 10% (v/v) FBS plus 0.1% (v/v) insulin, 1% (v/v) isobutylmethylxanthine and 0.1% (v/v) dexamethasone for 3 days. After that, the differentiation medium was changed to the maintenance medium (DMEM/10% FBS/0.1% insulin) for five more days until cells reach their terminal differentiation (verified by lipid droplet accumulation).

Plasma treatment and infection of 3T3-L1 cells

, Adipocytes were exposed to plasmas derived from control or infected mice (20% mouse plasma in DMEM). Plasmas were obtained by centrifugation at 5000 rpm during 20 min to avoid the presence of parasites. In addition, adipocytes were infected with trypomastigotes (MOI 20:1). In both cases, 48 h after the exposition to plasmas or parasites, culture dishes were washed with PBS, coverslips were removed for further fluorescence microscopy processing and adherent adipocytes were resuspended in TRI Reagent® for RT-qPCR.

Evaluation of 3T3-L1 differentiation by lipid droplet fluorescent staining

For fluorescence microscopy, 3T3-L1 adipocytes grown on coverslips were fixed with 4% paraformaldehyde for 15 min at room temperature. After washing with PBS, the coverslips were covered 10 min with 40,6-diamidino-2-phenylindole (DAPI; Invitrogen) for nuclei staining. Next, lipid droplets were stained with HCS LipidTOX™ Green Neutral Lipid Stains (Invitrogen) for 30 min and mounted with Fluorsafe (Millipore). Samples were analyzed by confocal microscopy using a Nikon C1 plus Eclipse TE-2000-E2 (Nikon, Melville, NY, USA), and the images obtained were subsequently analyzed using the Image J software (Bethesda, Maryland, USA).

Determination of macrophage phagocytic capacity

The phagocytosis assay was performed using heat-killed *Saccharomyces cerevisiae*. Yeasts were killed by heating in a water bath at 70–75 °C for 3 h as described in Capilla et al. [34]. Seventeen days pi, peritoneal macrophages were obtained from PPAR-γ agonist-treated animals, or not, and cultured in eight-well plates (Lab-Tek™ chamberslide, NUNC) overnight at a concentration of 30,000 cells/well. Cells were then incubated with yeast at a 10:1 ratio (yeast per cell) at 37 °C. After 2 h, the medium was removed, cells were washed twice with PBS and fixed with cold 70% ethanol. Finally, hematoxylin–eosin staining was performed. The phagocytic capacity was determined according to the amount of yeasts present inside the macrophages. Yeast was detected as oval intracytoplasmic structures characterized by a central eosinophilic nucleus surrounded by clear space (phagocytic vacuole). The phagocytic capacity was classified as: (1) null: zero yeast/cell, (2) low: up to five yeasts/cell, (3) high: more than five yeasts/cell. Ten fields/well were evaluated (recording at least 50 phagocytic cells).

Statistical analysis

Depending on the characteristics of the variable, differences in quantitative measurements were assessed by ANOVA followed by Bonferroni test or by the Kruskal–Wallis followed by post hoc comparisons when applicable. Results were expressed as mean ± standard error of the mean (SEM) unless otherwise indicated. The Graph-Pad Instat 5.0 software (Graph-Pad, California, USA) was applied for statistical analyses, and differences were considered significant when p value was < 0.05.

Results

Characterization of immuno-metabolic profile of acute *T. cruzi*-infected mice

First, to assess the immune–metabolic profile developed by C57BL/6 male mice along the course of *T. cruzi* acute infection, we evaluated several parameters related with inflammation and metabolism. As seen in Table 1, systemic inflammation and the severity of myocarditis clearly paralleled metabolic alterations, including the development of severe hypoglycemia and the dramatic loss of body weight as the most salient findings. Strikingly, infected animals did not lose their ability to handle glucose, judging from the results

Table 1 Immuno-metabolic profile of acute *T. cruzi*-infected male mice

	Days post-infection			
	0	14	17	21
Parasitological and histopathological parameters				
Parasitemia	–	32 (4–61)*	201 (129–360)*	391 (131–588)*
Myocarditis	–	Mild	Moderate	Severe
CPK	220 ± 26	795 ± 220*	1030 ± 549*	ND
Immunological parameters				
TNF (pg/ml)	0 ± 0	255 ± 16*	622 ± 50*	816 ± 116*
IL-6 (pg/ml)	0 ± 0	189 ± 5*	580 ± 80*	ND
IL-1β (pg/ml)	0 ± 0	33 ± 4*	74 ± 6*	102 ± 10*
Metabolic parameters				
Body weight (g)	31 ± 0.2	30 ± 0.5	26 ± 0.7*	22 ± 0.2*
Food intake (g/day/mice)	4.0 ± 0.1	3.1 ± 0.1*	2.8 ± 0.1*	2.4 ± 0.2*
Glycemia (mg/dl)	130 ± 10	102 ± 8*	69 ± 4*	48 ± 7*
Triglyceridemia (mg/dl)	105 ± 2	ND	135 ± 5*	178 ± 12*
Cholesterolemia (mg/dl)	127 ± 3	ND	154 ± 3*	168 ± 16*
Leptin (pg/ml)	64 ± 10	20 ± 3*	15 ± 2*	6 ± 0.5*

Immuno-metabolic parameters in control (0 dpi) and infected mice after 14, 17 and 21 dpi. Parasitemia, acute myocarditis degree and levels of creatine phosphokinase (CPK) were registered to characterize the systemic repercussion of acute *T. cruzi* infection. Plasma levels of key cytokines such as TNF, IL-6 and IL-1β were evaluated by ELISA. Metabolic characterization was based on: body weight changes, food intake abnormalities, glycemia, triglyceridemia, cholesterolemia and leptin circulating levels. $*p < 0.05$. Except for parasitemias (median, 25–75 percentiles), data correspond to mean ± SEM of five mice/group (one representative of three independent sets of experiments)

of glucose tolerance tests (Online Resource 2a). Likewise, the loss of body weight was directly associated with the decrease in circulating leptin levels, and to a lesser extent to a decreased food intake. During infections, the loss of body weight is often associated with the action of TNF [35]. To assess whether TNF was responsible for body weight loss during *T. cruzi* infection, TNF receptors 1 and 2 knockout mice were infected (Online Resource 2b).

Our results showed that these mice also lost weight, similar to wild-type mice, indicating that other factors are also involved in this process.

The infection with *T. cruzi* promotes a pro-inflammatory state in the AT and downregulates lipolytic and lipogenic pathways

The marked loss of body weight during the acute infection (~ 15–20% after 17 days pi, see Table 1) clearly reflected the reduction of AT mass, particularly the epididymal AT which constitutes the most abundant white fat pad in male mice. The parasitemia began to be detectable nearly 10 days pi. One week later (17 days pi), there was a dramatic diminution in the mass of the epididymal AT (Fig. 1a, b). This alteration was the result of a diminution in both size and number of adipocytes (Fig. 1c, d). The fall in the number of adipocytes may be consequence of an increased cell death, due to the presence of inflammation or by adipocyte lysis caused by parasite replicative forms. Adipocytes can act as a *T. cruzi* reservoir, persisting there for long periods of time. In fact, we found amastigote nests in the EAT of infected mice (Fig. 1d, right panel, see arrow). While inflammatory cells were not evident in the EAT from control animals, a noticeable inflammatory infiltrate was found in the EAT from infected mice (Fig. 1d, middle panel). As determined by flow cytometry (Fig. 1e, f), the EAT from infected mice revealed an increased percentage of T lymphocytes ($CD4^+$ and $CD8^+$ T cells), macrophages ($CD11b^+$) dendritic cells ($CD11c^+$) cells and dendritic-like cells ($CD11b^+CD11c^+$) compared to EAT from uninfected mice compared to uninfected AT (Fig. 1f). Conversely the percentage of Tregs ($CD4^+Foxp3^+$) was decreased in infected mice (Fig. 1f).

The diminution in the AT mass was paralleled by the development of hyperlipidemia evidenced by the increase in the level of circulating cholesterol and triglycerides (Fig. 2a). Additionally, LDL/HDL ratio was remarkably increased (Fig. 2b), probably contributing to an initial pro-atherogenic state. This hyperlipidemic state along with the diminution in the AT mass suggested an alteration in the lipolysis/lipogenesis balance. To evaluate this hypothesis, we assessed the mRNA expression of the main lipolytic (ATGL and HSL) and lipogenic enzymes (FAS, LPL, DGAT1 and DGAT2) in the epididymal AT of normal and infected mice. Surprisingly, we found a marked decrease

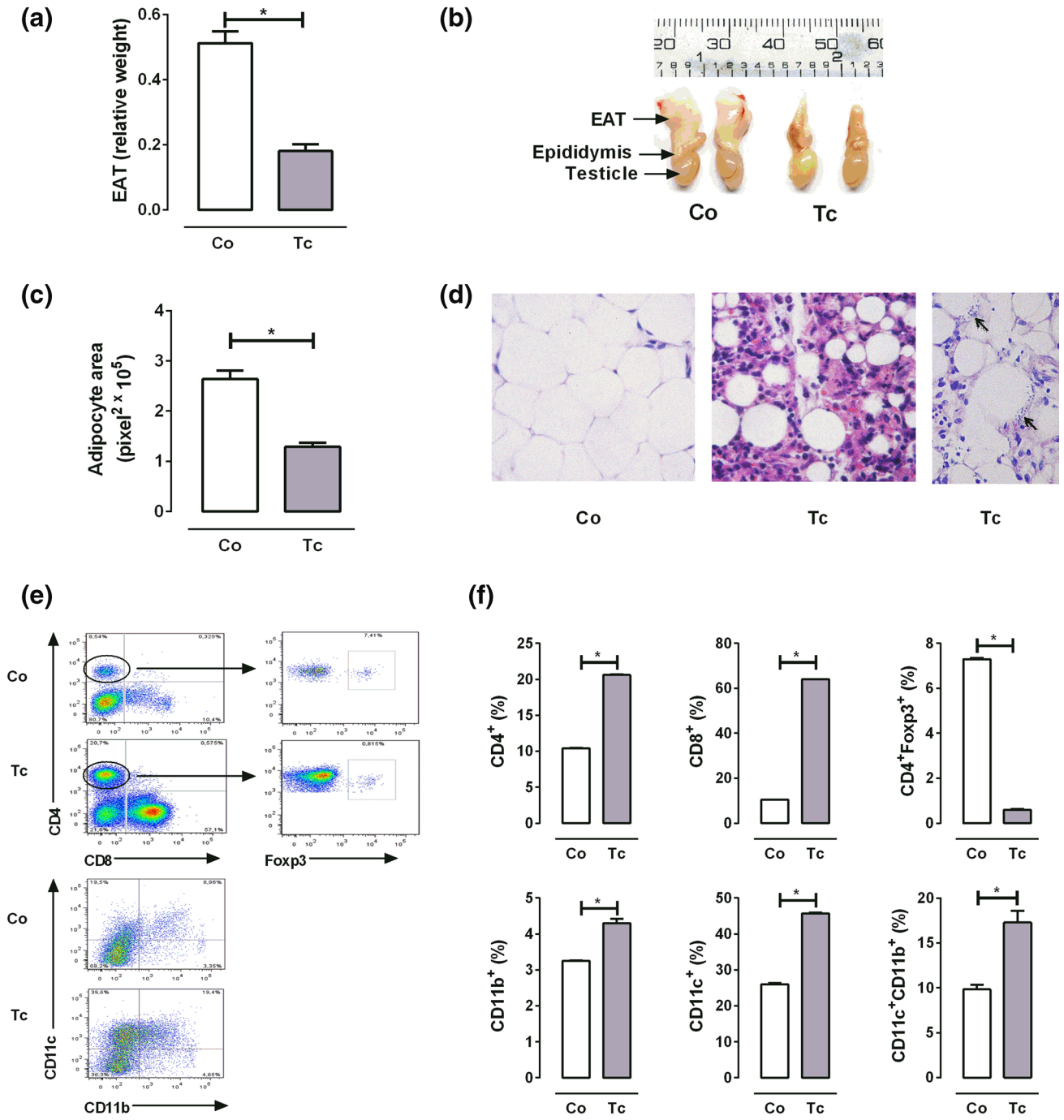

Fig. 1 Evaluation of adipose tissue after 17 dpi. Groups of non-infected (Co) or infected mice with *T. cruzi* (Tc) were euthanized and epididymal adipose tissue (EAT) was obtained. **a** EAT relative weight (EAT g/mice weight g). **b** Photography showing the loss of adipose tissue mass in infected mice. **c** Adipocyte area quantification. **d** Light microscopy photography of sections stained with hematoxylin and eosin. *Co* representative image of normal EAT architecture, *Tc* representative images of EAT of infected mice that shows the presence of large inflammatory infiltrate and intracellular parasite nests (black arrows); all images have a ×40 magnification. After 17 dpi, adipose tissue was processed to separate stromal vascular fraction cells (SVFC) for flow cytometry analysis. **e** Upper panel shows representative dot plots obtained by flow cytometry showing CD4+ and CD8+ gathered among total SVFC- and Foxp3-expressing cells among CD4+ subpopulation. Lower panels show gates used to identify the proportion of macrophages (CD11b+) and dendritic cells (CD11c+) from total SVFC. **f** Frequency of different immunological cell subpopulations among SVFC of adipose tissue. Data correspond to mean ± SEM of five mice/group (one representative of three independent sets of experiments). $*p < 0.05$

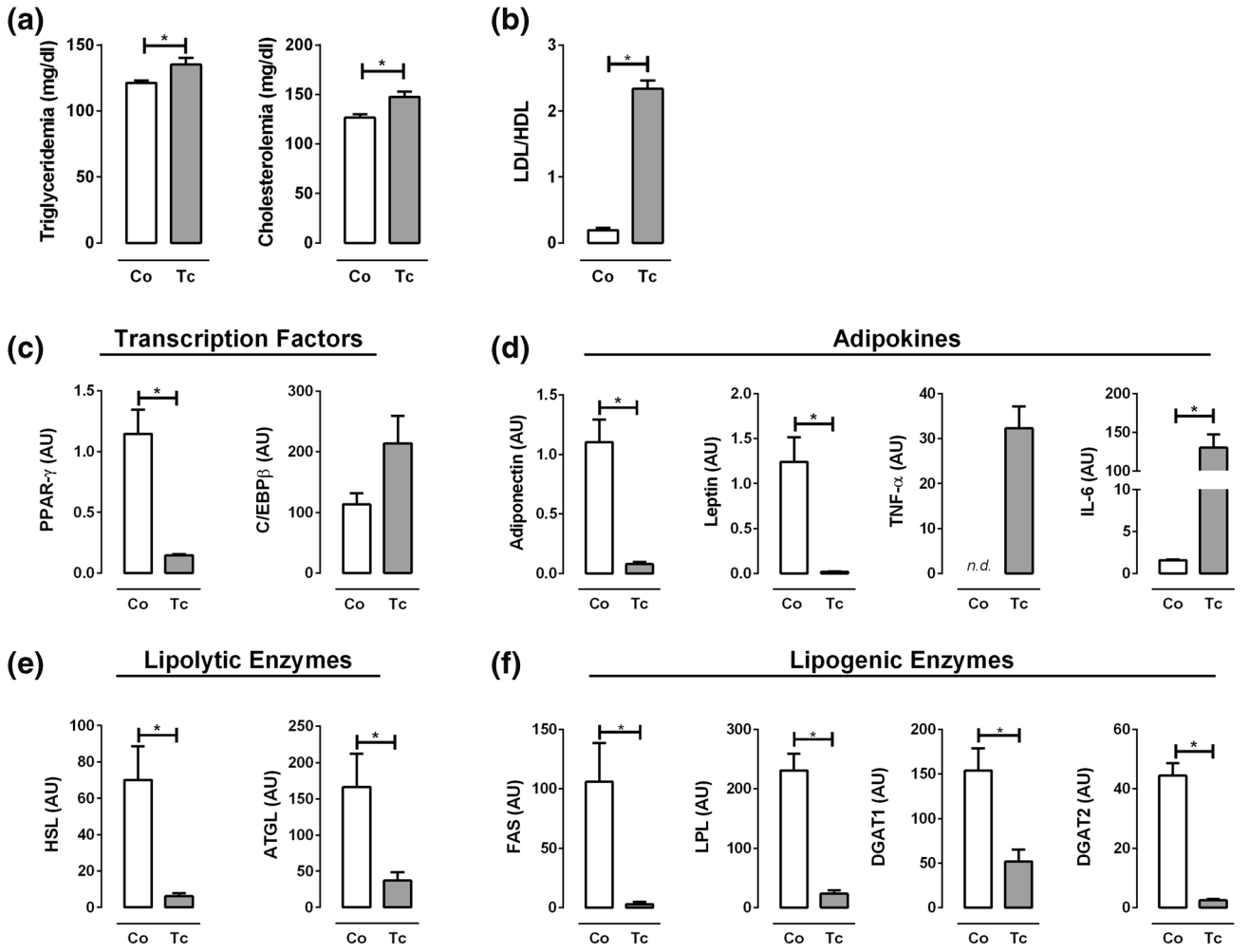

Fig. 2 Analysis of plasma lipid profile and mRNA expression of typical enzymes, transcription factors and adipokines in AT. After 17 dpi, plasma and adipose tissues were obtained from control (Co) and infected (Tc) mice. **a** Triglyceridemia and cholesterolemia. **b** LDL/HDL ratio. mRNA was extracted from EAT and quantitative real-time RT-PCR was performed for: **c** the transcription factors PPAR-γ and C/EBPβ; **d** the adipokines adiponectin, leptin, TNF and IL-6; **e** the lipolytic enzymes hormone-sensitive lipase (HSL) and adipose triglyceride lipase (ATGL); **f** the lipogenic enzymes fatty acid synthase (FAS), lipoprotein lipase (LPL) and diglyceride acyltransferase 1 and 2 (DGAT). *AU* arbitrary units. Data correspond to mean ± SEM of five mice/group (one representative of three independent sets of experiments). $^{*}p < 0.05$

in the expression of both lipolytic (Fig. 2e) and lipogenic enzymes (Fig. 2f), showing that both adipocyte catabolic and anabolic pathways are disrupted by the infection.

Furthermore, we also evaluated the expression of the main factors involved in adipogenesis, maintenance of adipocyte mature phenotype and inflammatory response: PPAR-γ and C/EBPβ transcription factors together with some adipokines. PPAR-γ expression was markedly diminished in the epididymal AT during acute infection, whereas C/EBPβ expression tended to increase (Fig. 2c). Adipokine expression was also affected, since mRNA levels of adiponectin and leptin were diminished in the infected EAT compared to normal EAT, while TNF and IL-6 were notoriously increased (Fig. 2d).

Given that EAT from infected mice was highly infiltrated by immune cells and only few adipocytes remained, we hypothesized that the reduction in the expression of adipocytes distinctive genes could be the result of an imbalance in the proportion of adipocytes/leukocytes. Therefore, to assess whether these changes corresponded specifically to an adipocyte expression pattern, we isolated mature adipocytes and the stromal vascular fraction cells (SVFC) by collagenase digestion and evaluated them separately (scheme). SVFC isolated from infected tissue exhibited a decrease level of PPAR-γ expression and a markedly increase in TNF expression indicating an inflammatory status of SVFC fraction (Fig. 3a, b). In line with the results obtained with infected EAT, isolated adipocytes

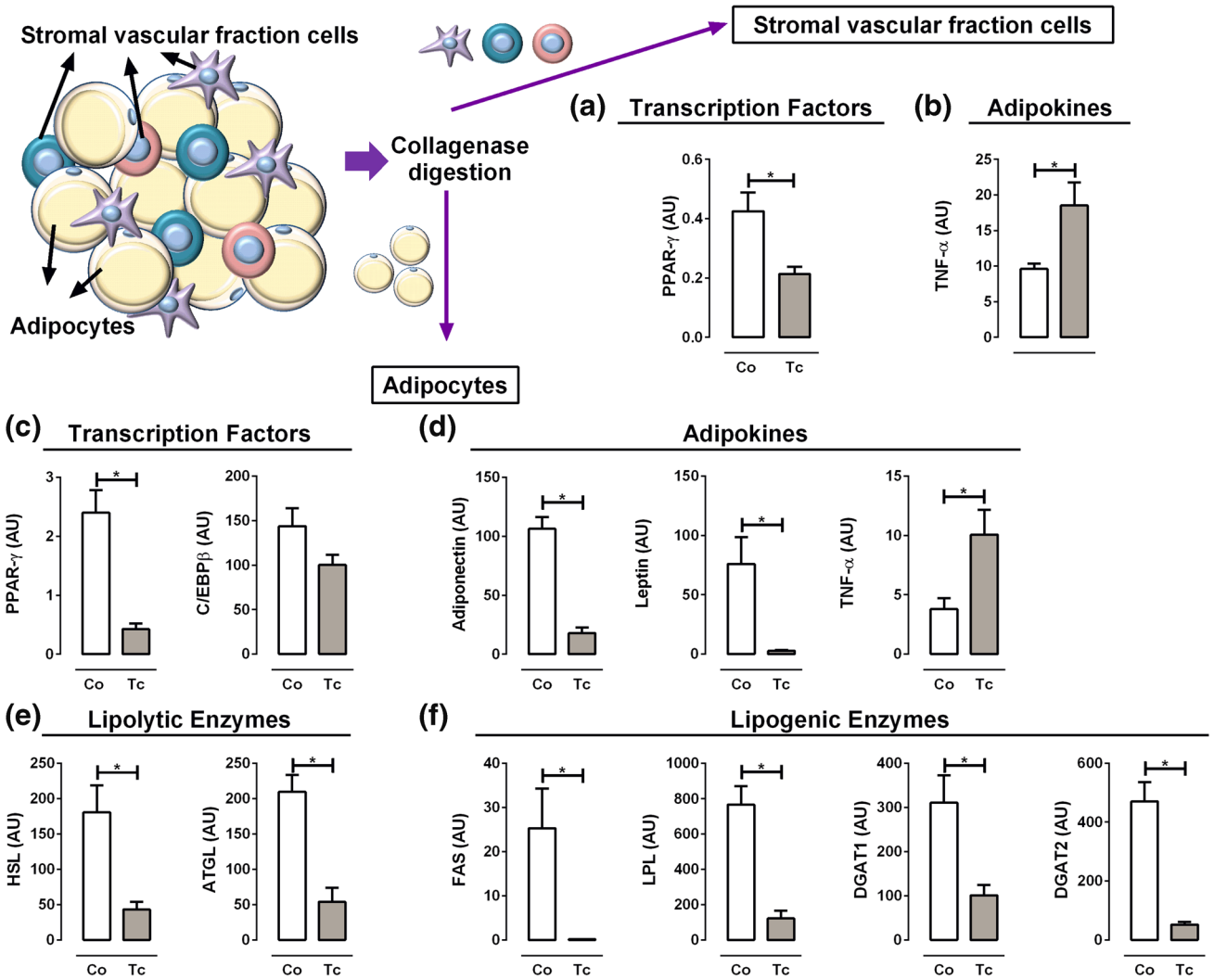

Fig. 3 Analysis of expression of typical enzymes, transcription factors and adipokines in stromal vascular fraction cells and adipocytes. After 17 dpi, the adipose tissue was extracted from control (Co) and infected (Tc) mice, and digested with collagenase to separate stromal vascular fraction cells and adipocytes. mRNA was extracted from each fraction of cells separately and quantitative real-time RT-PCR was performed. **a** PPAR-γ and **b** TNF expressions in stromal vascular fraction cells. Adipocyte expression of: **c** transcription factors PPAR-γ and C/EBPβ; **d** adipokines adiponectin, leptin and TNF-α; **e** lipolytic enzymes hormone-sensitive lipase (HSL) and adipose triglyceride lipase (ATGL); **f** lipogenic enzymes fatty acid synthase (FAS), lipoprotein lipase (LPL) and diglyceride acyltransferase 1 and 2 (DGAT). *AU* arbitrary units. Data correspond to mean ± SEM of five mice/group (one representative of three independent sets of experiments). $^*p < 0.05$

also showed decreased expression of PPAR-γ, adiponectin and leptin in concert with an enhanced expression of TNF (Fig. 3c, d), pointing out to a clear acquisition of an inflammatory phenotype. Noticeably, the reduction in lipolytic and lipogenic enzyme expressions was also confirmed (Fig. 3e, f). Hence, infection evidently disturbs adipocyte lipid metabolism, wherein the most affected process seems to be lipid storage leading to adipocyte atrophy and size diminution. Moreover, since PPAR-γ is diminished in SVFC, it is possible that de novo adipogenesis could be also affected.

Factors released during infection downregulate DGAT expression and promote the loss of mature phenotype of 3T3-L1 adipocyte in vitro

It is possible that soluble factors released by immune cells during *T. cruzi* infection affect AT homeostasis, independently of the *T. cruzi* presence. On the other hand, the parasite itself may influence directly AT atrophy. To evaluate these possibilities, a series of in vitro studies were carried out using the 3T3-L1 adipocytes (Fig. 4a). Initially, these cells were exposed during 48 h to plasmas derived from control (Co Pl) or infected (Tc Pl) mice. We observed that plates with 3T3-L1 adipocytes

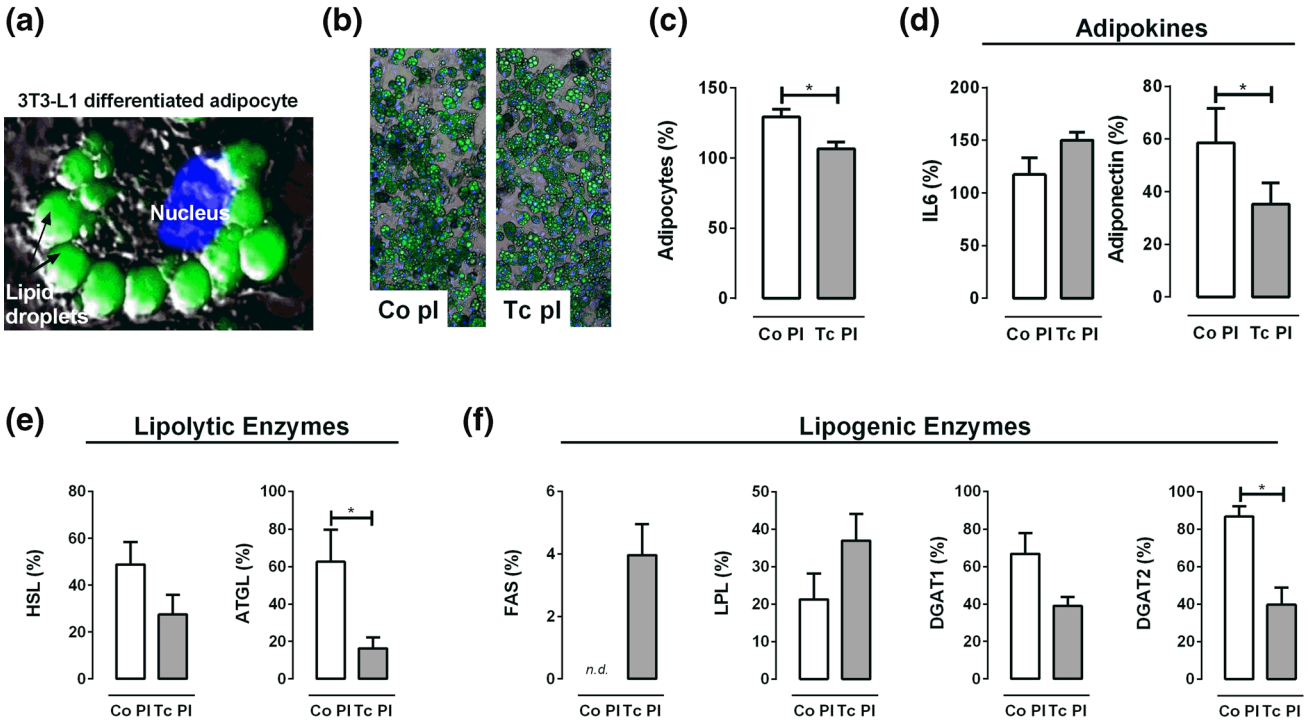

Fig. 4 Evaluation of fully differentiated 3T3-L1 adipocytes after 48-h exposure to plasmas from control (Co pl) and infected (Tc pl) mice. In vitro fully differentiated adipocytes were exposed to Co and Tc plasmas for 48 h. Control plates without plasma treatment were also cultured for 48 h. After that, adipocytes were stained for immunofluorescence analysis or resuspended in Tri-reagent for RT-qPCR. Results are relativized to values obtained in control cells without plasma treatment. **a** Representative immunofluorescence image showing a fully differentiated adipocyte. Lipid droplets were stained with LipidTox (green) and nuclei with DAPI (blue). **b** Pictures show immunofluorescence image of cultured adipocytes after exposure to Co and Tc plasmas. **c** Percentage of adipocytes present after exposure to Co and Tc plasmas. **d** Expression of adipokines adiponectin and IL-6. **e** Expression of lipolytic enzymes hormone-sensitive lipase (HSL) and adipose triglyceride lipase (ATGL). **f** Expression of lipogenic enzymes fatty acid synthase (FAS), lipoprotein lipase (LPL) and diglyceride acyltransferase 1 and 2 (DGAT). Data are represented as mean ± SEM of five mice/group (one representative of four independent sets of experiments). $^{*}p < 0.05$

treated with Co Pl presented a slightly higher percentage of adipocytes than cells treated with Tc Pl (Fig. 4b, c), suggesting that inflammatory factors released in circulation during infection may cause adipocyte death and/or adipocyte phenotype loss. IL-6 mRNA levels tended to increase while adiponectin levels diminished (Fig. 4d). Importantly, lipolytic enzyme ATGL, as well as the enzyme of the lipogenic pathway DGAT2 decreased their level of expression in 3T3-L1 adipocytes exposed to plasma derived from *T. cruzi*-infected mice (Fig. 4e, f), as observed in vivo in EAT (Fig. 2e, f). Since DGAT2 function is the limiting step required for lipid droplet formation, the decrease of it expression may possibly explain the loss of 3T3 cells in response to inflammatory mediators released during infection.

Infection with *T. cruzi* also affects adipocytes homeostasis in vitro

To study how *T. cruzi* parasite may affect the adipocyte by itself without interference of components from the host immune response, we infected in vitro 3T3-L1 adipocytes during 48 h. We observed a large number of amastigotes surrounding lipid droplets in the adipocyte (Fig. 5a, see arrows). As seen in vivo and in 3T3-L1 exposed to Tc-derived plasmas, the infection of 3T3-L1 adipocytes caused a markedly increased expression of IL-6 and TNF while adiponectin level of expression was reduced (Fig. 5b). Further, both lipolytic ATGL and lipogenic DAGT2 enzymes were also markedly decreased (Fig. 5c, d). No changes were detected in HSL, FAS and LPL enzymes but, in line with in vivo findings, all of them showed a tendency to decrease (Fig. 5c, d). Thus, in vitro *T. cruzi* infection strongly stimulates adipocyte production of inflammatory factors downregulating metabolic enzymes.

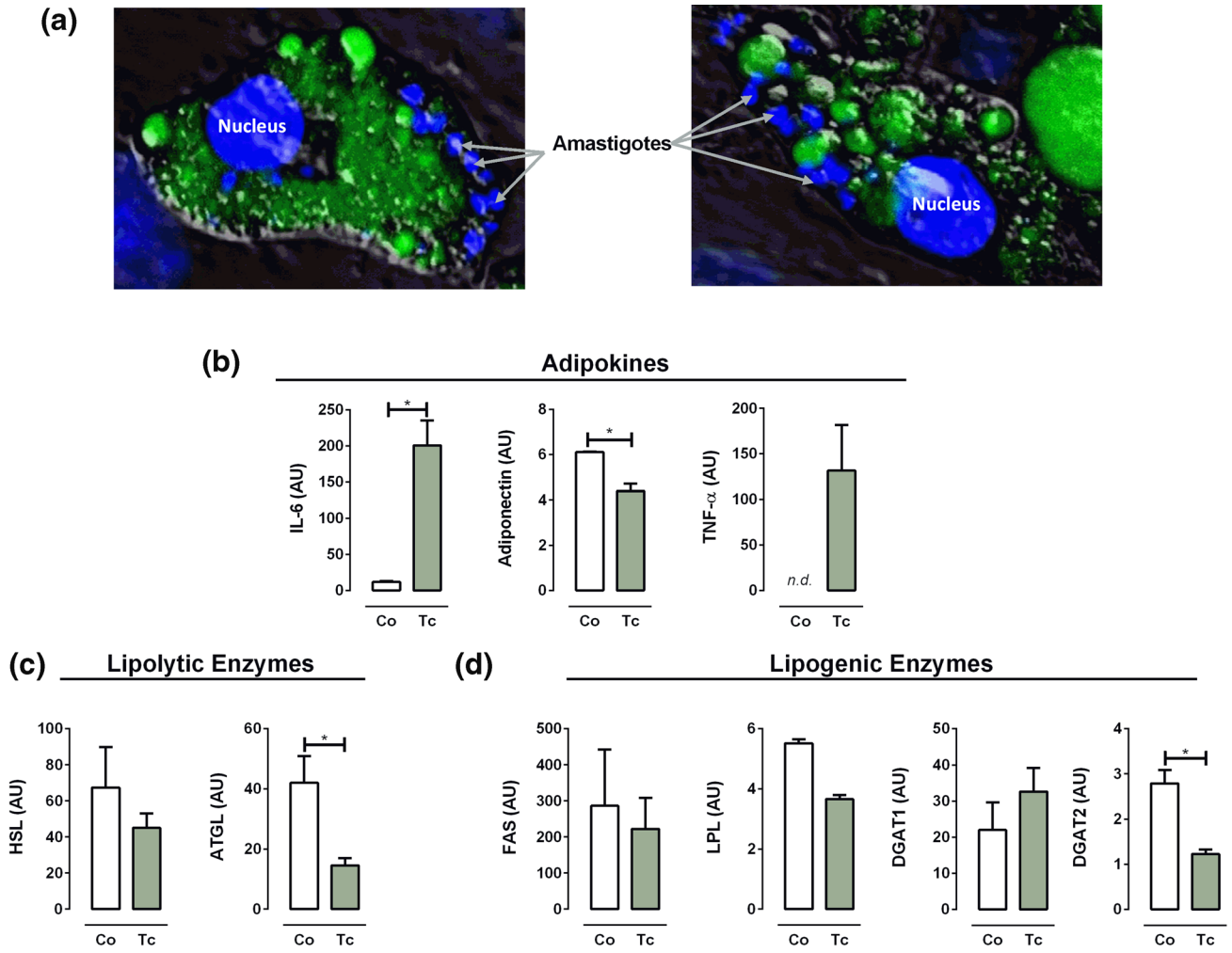

Fig. 5 In vitro infection of fully differentiated 3T3-L1 adipocytes. Adipocytes were infected with *T. cruzi* for 48 h. After that, cultured adipocytes were stained for immunofluorescence analysis or resuspended in Tri-reagent for RT-qPCR. **a** Immunofluorescence staining shows adipocytes (nucleus, blue; lipid droplets, green) containing intracellular amastigotes (small blue dots). **b** Expression of adipokines adiponectin, TNF and IL-6 in adipocytes. **c** Expression of lipolytic enzymes hormone-sensitive lipase (HSL) and adipose triglyceride lipase (ATGL) in adipocytes. **d** Expression of lipogenic enzymes fatty acid synthase (FAS), lipoprotein lipase (LPL) and diglyceride acyltransferase 1 and 2 (DGAT) in adipocytes. *Co* non-infected adipocytes, *Tc* infected adipocytes, *AU* arbitrary units. Data correspond to mean ± SEM of five mice/group (one representative of three independent sets of experiments). *$p < 0.05$

In vivo treatment with PPAR-γ agonist partially reestablishes metabolic features but fails to control the inflammatory response in AT during *T. cruzi* infection

Given the central role of PPAR-γ in energy homeostasis and inflammation, we attempted to improve the immunometabolic response using PPAR-γ agonists. Therefore, we evaluated whether the daily administration of 15-dPGJ2 (PGJ) or rosiglitazone (Rsg) (Fig. 6a) was able to decrease inflammation as well as normalize metabolic factors and enzyme expression in EAT. It is well known that PPAR-γ agonist induces weight gain [36, 37]. Nevertheless, both agonists neither affected the weight of Co animals nor modified the curve of weight loss recorded during infection (data not shown). Rsg treatment partially prevented adipocyte size diminution (Fig. 6b) or tissue immune infiltration (Fig. 6c). In contrast, PGJ administration blocked the loss of lipid droplets (Fig. 6b) and drastically diminished the presence of inflammatory infiltrate (Fig. 6c). Surprisingly, the proportion of macrophages among the inflammatory infiltrate was augmented (Online Resource 2c). It is known that PPAR-γ agonists induce macrophage polarization towards an anti-inflammatory phenotype in parallel with a diminution of their phagocytic capacity [38, 39]. Coincidently, in vivo Rsg or PGJ treatment reduced phagocytic capacity and induced the acquisition of a foamy-like phenotype in peritoneal macrophages (Online Resource 2d

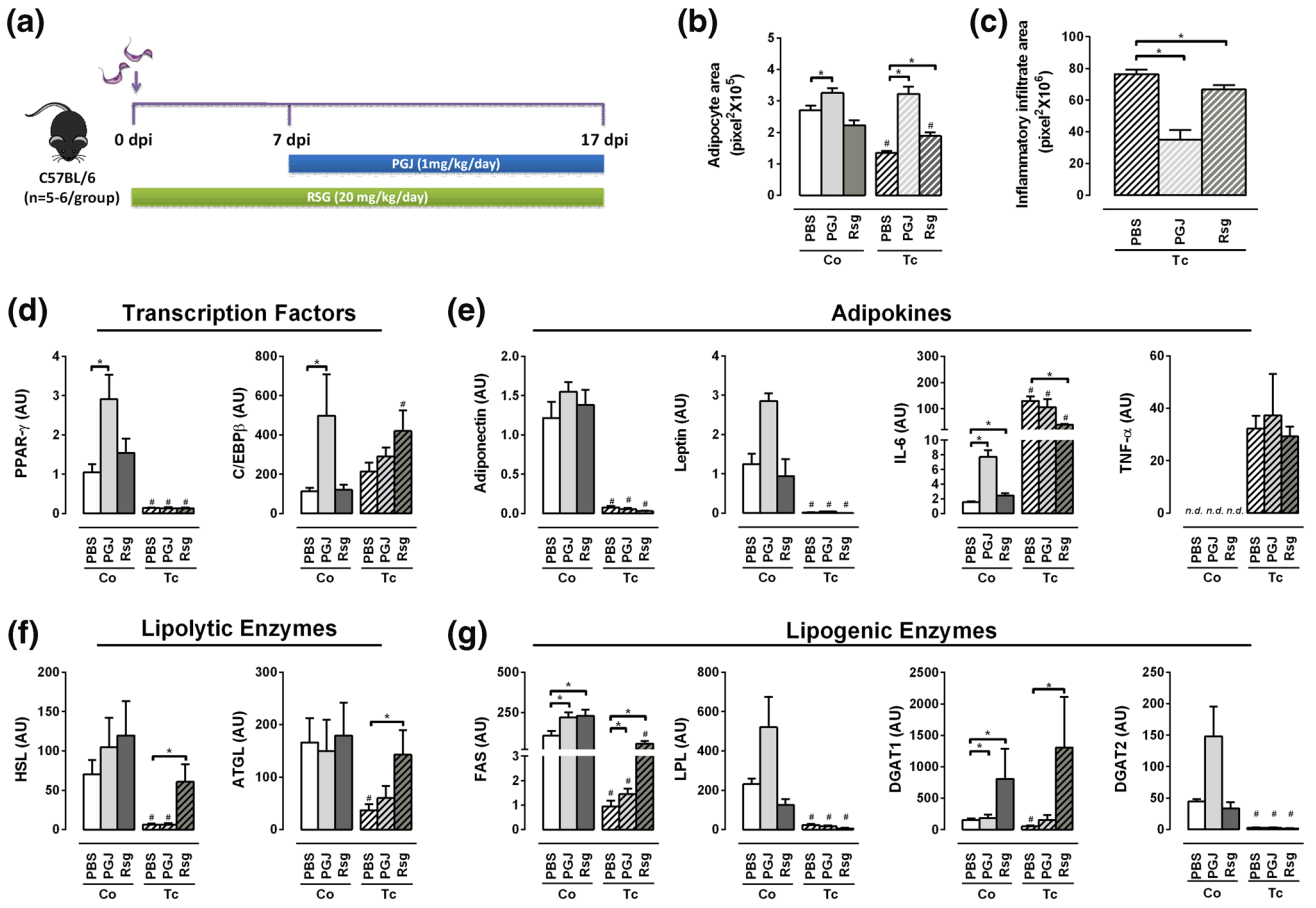

Fig. 6 Evaluation of effects on adipose tissue of PPAR-γ agonist treatment during infection. **a** Control (Co) and infected mice (Tc) were treated with the PPAR-γ agonists rosiglitazone (Rsg) and 15-deoxy-Δ12,14-prostaglandin J2 (PGJ) during acute infection. After 17 dpi, mice were sacrificed, adipose tissue extracted and used for histopathological examination or RT-qPCR. Quantification of **b** adipocyte area and **c** inflammatory infiltrate area by image analysis. mRNA was extracted from EAT and quantitative real-time RT-PCR was performed for: **d** transcription factors PPAR-γ and C/EBPβ in adipocytes; **c, e** adipokines adiponectin, leptin, IL-6 TNF-α; **d, f** lipolytic enzymes hormone-sensitive lipase (HSL) and adipose triglyceride lipase (ATGL); **e, g** lipogenic enzymes fatty acid synthase (FAS), lipoprotein lipase (LPL) and diglyceride acyltransferase 1 and 2 (DGAT) in adipocytes. *AU* arbitrary units. Data correspond to mean ± SEM of five mice/group (one representative of three independent sets of experiments). $^{*}p < 0.05$. $^{\#}p < 0.05$ respect to corresponding Co group

and 2e), raising the possibility that macrophages in AT may acquire a similar pattern when PPAR-γ agonist was administered to infected mice.

Next, we examined the effect of Rsg or PGJ treatments on mRNA levels of adipocyte-specific genes. In control mice, only PGJ treatment increased the level of PPAR-γ and C/EBPβ mRNAs (Fig. 6d). In infected mice, C/EBPβ mRNA was increased only by Rsg treatment while the decrease of PPAR-γ expression could not be prevented by PGJ or Rsg treatment (Fig. 6d), suggesting that inflammatory mediators released by the immune response may possibly suppress PPAR-γ expression regardless of agonist administration. No differences were observed in the expression of adiponectin, leptin or TNF after treatments neither in control nor infected mice (Fig. 6e). Interestingly, IL-6 expression was upregulated in control mice and only slightly diminished in infected mice treated with Rsg. Overall, these results showed that agonist treatments failed to cope with EAT inflammation and PPAR-γ expression.

Regarding lipolytic enzymes HSL and ATGL, Rsg but not PGJ treatment restored their expression in infected mice (Fig. 6f). Lipogenic enzymes FAS and DGAT1 were upregulated by PGJ or Rsg in control animals (Fig. 6g), indicating that the novo fatty acid and triglyceride synthesis are stimulated. The same pattern was observed in LPL and DGAT2 in PGJ-treated and control animals (Fig. 6g). Moreover, both agonist upregulated FAS expression in infected mice, while Rsg alone increased DGAT1 in the same group (Fig. 6g). Taken together, these results suggest that Rsg treatment throughout *T. cruzi* infection favors the expression of both lipolytic and lipogenic enzymes, resulting in a partial improvement of adipocyte size and diminished

inflammatory infiltrates, thus favoring the restoration of the metabolic homeostasis of adipocyte.

Discussion

Herein, we demonstrated that experimental *T. cruzi* infection affects WAT homeostasis and adipocyte functionality. During *T. cruzi* infection, we observed a markedly catabolic situation, with loss of AT and adipocyte atrophy, implying an increased lipolysis rate, probably triggered by inflammatory mediators. TNF have been described as a main promoter of lipolysis and coincidentally C57BL/6-infected mice display higher tissue and circulating levels of this cytokine [25, 28, 40]. One mechanism proposed for this effect is that TNF promotes perilipin phosphorylation, and consequently accelerates lipid hydrolysis [41]. Nevertheless, we previously showed that infected mice in which TNF signalling is totally blocked (TNF-$R_{(1+2)}$KO mice) develop a clear clinic affectation [42]. Considering our reports here indicating that infected TNF-$R_{(1+2)}$KO mice loss AT mass at a similar level that infected Co ones, we speculated that AT loss may be also caused synergistically by other factors such as IL-1β or IL-6, which are also strongly elevated in infected mice [42–45]. Moreover, since stress response is activated in *T. cruzi*-infected C57BL/6 mice [46, 47], the release of catecholamines in situ might also synergize the lipolytic effect [48].

Contrary to what was expected, the expression of the main lipolytic enzymes was sharply downregulated in vivo (as seen in Figs. 2e, 3e). Additionally, cultured 3T3-L1 adipocytes showed the same pattern when exposed to plasma of infected mice that carried factors released by immune response against *T. cruzi* or infected in the absence of host-released immune mediators (as seen in Figs. 4e, 5c). Furthermore, since TNF was shown to downregulate the expression of ATGL and HSL possibly due to PPAR-γ inhibition [49–51], it can be speculated that TNF may be responsible, in part, for ATGL and HSL decreased expression during in vivo *T. cruzi* infection. The fall in the expression of both lipolytic enzyme genes may be the result of a clear establishment of infection (high parasitemia and clinic involvement); since differing from our results, Nagajyothi et al. [31] found an increase of HSL by western blot at an early infection phase, before the appearance of the parasite in blood and clinical signs of infection, while ATGL expression is sharply depressed. Nevertheless, independently of HSL levels, the loss of ATGL expression might be difficult the first step of the lipolytic pathway, causing the diminution of diacylglycerol, the substrate of HSL.

In vivo *T. cruzi* infection also affects profoundly the expression of enzymes involved in lipogenesis, suggesting that critical steps in the triglyceride synthesis are compromised. In addition, the mRNA of DGAT2, enzyme that catalyzes the final and critical step in the triglyceride deposition within adipocytes, is also significantly reduced in vitro. These findings indicate that the decrease in adipocyte size may reflect their inability to store lipids. Additionally, triglyceride store diminution may be a consequence of reduced the novo fatty acid synthesis or a decrease in their intake, phenomena which may be strongly influenced by FAS and LPL downregulation. In fact, hypertriglyceridemia observed in infected mice may be the result of lipogenic pathway dysfunction and the consequent AT inability to store lipids, decreasing its clearance. Although there are no other publications evaluating the effect of *T. cruzi* infection on FAS and DGAT, comparable results have been observed in diverse infections and endotoxemia models [52–55]. Strikingly, Nagajyothi et al. [31] showed in a murine model of *T. cruzi* infection, an enhancement of LPL protein in the pre-parasitemic phase, suggesting that the kinetic of infection may influence enzyme expression. Moreover, we cannot also rule out the possibility that the use of different strains of mice and parasite (CD1 and Brazil, respectively) can be involved in these differences. Thus, the downregulation of lipogenic enzymes, and the consequent dysfunction of the anabolic pathway, may be the result of an inhibitory action mediated by inflammatory cytokines such as TNF, IL-6 or IL-1β [56–59].

Overall, these results suggest that there is an imbalance between the lipolysis/lipogenesis rate. While lipolysis does not seem to be increased, there is a decrease in lipogenesis, so the inability of adipocytes to store fatty acids seems to be the main cause of AT atrophy. We can rule out that the loss of AT could be also partly due to the death of adipocytes because of the lysis caused by the intracellular parasite replication, by severe PPAR-γ downregulation [16] as well as by apoptotic signal triggered by the inflammatory response.

T. cruzi-derived molecules such as glycoinositolphospholipids (GPI) anchors and DNA can induce pro-inflammatory cytokine production in innate immune cells by stimulation of several Toll-like receptors (TLR), such as TLR-9, TLR-2 and TLR-4 [60, 61]. On the other hand, other series of studies showed that adipocytes express a wide range of TLRs and that their stimulation leads to the establishment of an inflammatory phenotype with production of IL-6 and TNF [62–66]. In this regard, Nagajyothi and co-workers [31, 67] found an upregulation of TLR-2, -4 and -9 in 3T3-L1 adipocytes and AT of mice infected with *T. cruzi*. Since we found an upregulation of IL-6 and TNF when adipocytes were infected in vitro, it may be speculated that TLR stimulation by *T. cruzi* induces the release of these cytokines, further inhibiting the expression of DAGT, ATGL and adiponectin in an autocrine/paracrine manner. Furthermore, given that

PPAR-γ is necessary for the maintenance of mature adipocyte phenotype [13–15], their noticeably in vivo downregulation appears to be responsible for the loss of expression of metabolic enzymes as well as adipokines and leading to the acquisition of an inflammatory phenotype defined by the secretion of TNF and IL-6. Reinforcing our results, a previous work dealing with cultured adipocytes infected with Tulahuén strain also showed an infection-associated diminution in the expression of PPAR-γ [67]. Strikingly, an enhancement in PPAR-γ protein and mRNA was reported in WAT during the pre-parasitic phase of *T. cruzi* infection [31], suggesting that PPAR-γ early activation constitutes a rapid response to inflammation. Nevertheless, our results showed that PPAR-γ expression seems to be actively inhibited when the acute phase becomes symptomatic and the parasite and pro-inflammatory immune mediators are clearly evidenced in blood.

Additionally, the clear decrease in factors that counter-regulate the inflammatory response in the AT, such as PPAR-γ, adiponectin and regulatory T cells, allow the establishment of severe inflammation during *T. cruzi* infection. In models of insulin resistance, PPAR-γ downregulation was shown to promote an increase in the proportion of M1-inflammatory macrophages infiltrating the AT; while its activation inhibited the release of inflammatory mediators [68, 69]. Coincidentally, macrophage and T-cell proportions were predominant in the AT of infected mice. Moreover, the expression of PPAR-γ in these infiltrating cells following isolation was clearly downregulated (as seen in Fig. 3a), indicating the prevalence of an inflammatory phenotype. Also, adiponectin decrease may favor inflammation, weakening the proportion of Tregs, as shown in adverse metabolic or autoimmune dysregulated contexts [70, 71]. In line with our results, adiponectin decrease seems to be a common feature of *T. cruzi* in vivo and in vitro infection models, indicating that is one of the most affected anti-inflammatory factors [29, 31, 67].

The beneficial effects of PPAR-γ agonist administration in inflammatory contexts have been well documented, especially regarding their inhibitory actions on pro-inflammatory cytokine secretion [72]. In fact, the protective role of PPAR-γ agonists in acute *T. cruzi* infection has been previously evaluated at cardiac tissue level and these findings suggested that they have antiflogistic effects [73–75]. Thus, we hypothesized that inducing PPAR-γ expression and activation using endogenous or synthetic agonists will act to reduce AT inflammation, therefore, improving lipid storage and consequently preventing adipocyte atrophy. Both agonists failed to counteract the expression of pro-inflammatory cytokines in infected animals; however, the inflammatory infiltrate was markedly reduced. Nevertheless, we would like to mention that both Rsg and PGJ exerted the expected effects in AT of control healthy animals. PPAR-γ can favor lipid storage in AT by stimulating lipogenic enzyme expression [76–80], a mechanism that may be the responsible for the weight gain observed after agonist treatment in animals and humans [36, 37]. Interestingly, even though Rsg failed to effectively counteract the inflammatory cytokine production or restore PPAR-γ expression, it did restore the expression of the lipolytic enzymes ATGL and HSL, and the lipogenic enzymes FAS and DGAT1. Overall, these results point out that agonist treatment partially reversed some of the metabolic imbalances found in AT of infected mice but was unable to efficiently control the inflammation at this level, suggesting a dissociation between PPAR-γ-mediated inflammatory and metabolic actions during infection.

The course of an infectious process has traditionally been regarded as the result of a host–parasite relationship in which defensive mechanisms, mostly immune-mediated, exerted a major role in pathogen resistance. Fruitful as it was, it is becoming clear that a series of non-competing processes, partly related to the immune response and microorganism presence also account for infection course and/or disease morbidity. Results from the present work indicate that experimental acute *T. cruzi* infection disrupts both adipocyte catabolic and anabolic metabolism secondary to PPAR-γ robust downregulation, tipping the balance towards to an adverse status compatible with the AT atrophy and the acquisition of an inflammatory phenotype. These severe metabolic alterations are much likely to affect the energetic demands dealing with the parasite control and the ensuing disease evolution.

Acknowledgements ARP, GPP, JT, LD, OAB and SRV are members of The National Council Research (CONICET). FBG thanks CONICET for a fellowship. JM thanks CIN (National Interuniversity Council) for a fellowship. This work was supported by grants from the Secretary of Sciences and Technology of National University of Rosario (SCYTUNR, 1MED-348 and 1MED-372), National Agency for Scientific and Technological Promotion (ANPCYT, PICT 2013-1892) and PIP-CONICET 0614. The authors thank Wiener Lab. Foundation for their help in supplying some laboratory reagents. We thank Farré Cecilia, Esdras da Silva Oliveira Barbosa and Cabral Nicolás by their technical assistance.

Compliance with ethical standards

Conflict of interest The authors declare that they have no conflict of interest.

Ethical approval The latest National Institute of Health guide for the care and use of laboratory was followed. The study was approved by the Institutional Animal Care and Use Committee of the School of Medicine of National University of Rosario by resolution no. 4977/2013.

References

1. Choe SS, Huh JY, Hwang IJ et al (2016) Adipose tissue remodeling: its role in energy metabolism and metabolic disorders. Front Endocrinol (Lausanne) 7:30
2. Kershaw EE, Flier JS (2004) Adipose tissue as an endocrine organ. J Clin Endocrinol Metab 89:2548–2556. https://doi.org/10.1210/jc.2004-0395
3. Halberg N, Wernstedt-Asterholm I, Scherer PE (2008) The adipocyte as an endocrine cell. Endocrinol Metab Clin N Am 37:753–768
4. Scherer PE (2016) The multifaceted roles of adipose tissue—therapeutic targets for diabetes and beyond: the 2015 banting lecture. Diabetes 65:1452–1461
5. Luo L, Liu M (2016) Adipose tissue in control of metabolism. J Endocrinol 231:R77–R99
6. Yen C-LE, Stone SJ, Koliwad S et al (2008) Thematic review series: glycerolipids. DGAT enzymes and triacylglycerol biosynthesis. J Lipid Res 49:2283–2301. https://doi.org/10.1194/jlr.R800018-JLR200
7. Wakil SJ (1989) Fatty acid synthase, a proficient multifunctional enzyme. Biochemistry 28:4523–4530. https://doi.org/10.1021/bi00437a001
8. Haemmerle G, Zimmermann R, Hayn M et al (2002) Hormone-sensitive lipase deficiency in mice causes diglyceride accumulation in adipose tissue, muscle, and testis. J Biol Chem 277:4806–4815. https://doi.org/10.1074/jbc.M110355200
9. Zimmermann R, Strauss JG, Haemmerle G et al (2004) Fat mobilization in adipose tissue is promoted by adipose triglyceride lipase. Science 306:1383–1386. https://doi.org/10.1126/science.1100747
10. Schweiger M, Schreiber R, Haemmerle G et al (2006) Adipose triglyceride lipase and hormone-sensitive lipase are the major enzymes in adipose tissue triacylglycerol catabolism. J Biol Chem 281:40236–40241. https://doi.org/10.1074/jbc.M608048200
11. Rosen ED, Spiegelman BM (2014) What we talk about when we talk about fat. Cell 156:20–44
12. Charó NL, Rodríguez Ceschan MI, Galigniana NM et al (2016) Organization of nuclear architecture during adipocyte differentiation. Nucleus 7:249–269
13. Tontonoz P, Spiegelman BM (2008) Fat and beyond: the diverse biology of PPARγ. Annu Rev Biochem 77:289–312. https://doi.org/10.1146/annurev.biochem.77.061307.091829
14. Tamori Y, Masugi J, Nishino N, Kasuga M (2002) Role of peroxisome proliferator-activated receptor-gamma in maintenance of the characteristics of mature 3T3-L1 adipocytes. Diabetes 51:2045–2055. https://doi.org/10.2337/diabetes.51.7.2045
15. Zhang B, Berger J, Hu E et al (1996) Negative regulation of peroxisome proliferator-activated receptor-gamma gene expression contributes to the antiadipogenic effects of tumor necrosis factor-alpha. Mol Endocrinol 10:1457–1466. https://doi.org/10.1210/mend.10.11.8923470
16. Imai T, Takakuwa R, Marchand S et al (2004) Peroxisome proliferator-activated receptor gamma is required in mature white and brown adipocytes for their survival in the mouse. Proc Natl Acad Sci USA 101:4543–4547. https://doi.org/10.1073/pnas.0400356101
17. Kim SR, Lee KS, Park HS et al (2005) Involvement of IL-10 in peroxisome proliferator-activated receptor gamma-mediated anti-inflammatory response in asthma. Mol Pharmacol 68:1568–1575. https://doi.org/10.1124/mol.105.017160
18. Ferreira AE, Sisti F, Sonego F et al (2014) PPAR-γ/IL-10 axis inhibits MyD88 expression and ameliorates murine polymicrobial sepsis. J Immunol 192:2357–2365. https://doi.org/10.4049/jimmunol.1302375
19. Choi JM, Bothwell ALM (2012) The nuclear receptor PPARs as important regulators of T-cell functions and autoimmune diseases. Mol Cells 33:217–222
20. Yang XY, Wang LH, Farrar WL (2008) A role for PPARgamma in the regulation of cytokines in immune cells and cancer. PPAR Res 2008:961753. https://doi.org/10.1155/2008/961753
21. Wang D, Shi L, Xin W et al (2017) Activation of PPARγ inhibits its pro-inflammatory cytokines production by upregulation of miR-124 in vitro and in vivo. Biochem Biophys Res Commun 486:726–731. https://doi.org/10.1016/j.bbrc.2017.03.106
22. Yang XY, H WL, Chen T et al (2000) Activation of human T lymphocytes is inhibited by peroxisome proliferator-activated receptor γ (PPARγ) agonists. J Biol 275:4541–4545
23. Miettinen S, Sarkanen JR, Ashammakhi N (2008) Adipose tissue and adipocyte differentiation: molecular and cellular aspects and tissue engineering applications. Top Tissue Eng 4:1–26
24. Lefterova MI, Zhang Y, Steger DJ et al (2008) PPARγ and C/EBP factors orchestrate adipocyte biology via adjacent binding on a genome-wide scale. Genes Dev 22:2941–2952. https://doi.org/10.1101/gad.1709008
25. Roggero E, Perez A, Tamae-Kakazu M et al (2002) Differential susceptibility to acute *Trypanosoma cruzi* infection in BALB/c and C57BL/6 mice is not associated with a distinct parasite load but cytokine abnormalities. Clin Exp Immunol 128:421–428. https://doi.org/10.1046/j.1365-2249.2002.01874.x
26. Roggero E, Pérez AR, Tamae-Kakazu M et al (2006) Endogenous glucocorticoids cause thymus atrophy but are protective during acute *Trypanosoma cruzi* infection. J Endocrinol 190:495–503. https://doi.org/10.1677/joe.1.06642
27. Tanowitz HB, Amole B, Hewlett D, Wittner M (1988) *Trypanosoma cruzi* infection in diabetic mice. Trans R Soc Trop Med Hyg 82:90–93
28. Manarin R, Villar SR, Bussy RF et al (2013) Reciprocal influences between leptin and glucocorticoids during acute *Trypanosoma cruzi* infection. Med Microbiol Immunol 202:339–352. https://doi.org/10.1007/s00430-013-0294-1
29. Combs TP, Nagajyothi J, Mukherjee S et al (2005) The adipocyte as an important target cell for *Trypanosoma cruzi* infection. J Biol Chem 280:24085–24094. https://doi.org/10.1074/jbc.M412802200
30. Matos Ferreira AV, Segatto M, Menezes Z et al (2011) Evidence for *Trypanosoma cruzi* in adipose tissue in human chronic Chagas disease. Microbes Infect 13:1002–1005. https://doi.org/10.1016/j.micinf.2011.06.002
31. Nagajyothi F, Desruisseaux MS, MacHado FS et al (2012) Response of adipose tissue to early infection with *Trypanosoma cruzi* (Brazil Strain). J Infect Dis 205:830–840. https://doi.org/10.1093/infdis/jir840
32. Zingales B, Andrade SG, Briones MRS et al (2009) A new consensus for *Trypanosoma cruzi* intraspecific nomenclature: second revision meeting recommends TcI to TcVI. Mem Inst Oswaldo Cruz. https://doi.org/10.1590/S0074-02762009000700021
33. Toneatto J, Guber S, Charo NL et al (2013) Dynamic mitochondrial-nuclear redistribution of the immunophilin FKBP51 is regulated by the PKA signaling pathway to control gene expression during adipocyte differentiation. J Cell Sci 126:5357–5368. https://doi.org/10.1242/jcs.125799
34. Capilla J, Clemons KV, Liu M et al (2009) Saccharomyces cerevisiae as a vaccine against coccidioidomycosis. Vaccine. https://doi.org/10.1016/j.vaccine.2009.03.030
35. Tracey KJ, Cerami A (1990) Metabolic responses to cachectin/TNF. A brief review. Ann N Y Acad Sci 587:325–331
36. Maudelonde T, Lluis F (2005) PPAR gamma ligands and the control of metabolism. Med Ther Med la Reprod 7:127–132

37. Larsen TM, Toubro S, Astrup A (2003) PPARgamma agonists in the treatment of type II diabetes: Is increased fatness commensurate with long-term efficacy? Int J Obes 27:147–161
38. Krysko O, Holtappels G, Zhang N et al (2011) Alternatively activated macrophages and impaired phagocytosis of *S. aureus* in chronic rhinosinusitis. Allergy Eur J Allergy Clin Immunol 66:396–403. https://doi.org/10.1111/j.1398-9995.2010.02498.x
39. Varin A, Mukhopadhyay S, Herbein G, Gordon S (2010) Alternative activation of macrophages by IL-4 impairs phagocytosis of pathogens but potentiates microbial-induced signalling and cytokine secretion. Blood 115:353–362. https://doi.org/10.1182/blood-2009-08-236711
40. Pérez AR, Tamae-Kakazu M, Pascutti MF et al (2005) Deficient control of *Trypanosoma cruzi* infection in C57BL/6 mice is related to a delayed specific IgG response and increased macrophage production of pro-inflammatory cytokines. Life Sci 77:1945–1959. https://doi.org/10.1016/j.lfs.2005.01.025
41. Zhang HH, Halbleib M, Ahmad F et al (2002) Tumor necrosis factor-α stimulates lipolysis in differentiated human adipocytes through activation of extracellular signal-related kinase and elevation of intracellular cAMP. Diabetes 51:2929–2935. https://doi.org/10.2337/diabetes.51.10.2929
42. Pérez AR, Roggero E, Nicora A et al (2007) Thymus atrophy during *Trypanosoma cruzi* infection is caused by an immunoendocrine imbalance. Brain Behav Immun 21:890–900. https://doi.org/10.1016/j.bbi.2007.02.004
43. Doerrler W, Feingold KR, Grunfeld C (1994) Cytokines induce catabolic effects in cultured adipocytes by multiple mechanisms. Cytokine 6:478–484. https://doi.org/10.1016/1043-4666(94)90074-4
44. Feingold KR (1992) Stimulation of lipolysis in cultured fat cells by tumor necrosis factor, interleukin-1, and the interferons is blocked by inhibition of prostaglandin synthesis. Endocrinology 130:10–16. https://doi.org/10.1210/en.130.1.10
45. Ji C, Chen X, Gao C et al (2011) IL-6 induces lipolysis and mitochondrial dysfunction, but does not affect insulin-mediated glucose transport in 3T3-L1 adipocytes. J Bioenerg Biomembr 43:367–375. https://doi.org/10.1007/s10863-011-9361-8
46. Roggero E, Pérez AR, Bottasso OA et al (2009) Neuroendocrine-immunology of experimental Chagas' disease. Ann N Y Acad Sci 1153:264–271
47. Roggero E, Perez AR, Pollachini N et al (2016) The sympathetic nervous system affects the susceptibility and course of *Trypanosoma cruzi* infection. Brain Behav Immun 58:228–236. https://doi.org/10.1016/j.bbi.2016.07.163
48. Duncan RE, Ahmadian M, Jaworski K et al (2007) Regulation of lipolysis in adipocytes. Annu Rev Nutr 27:79–101. https://doi.org/10.1146/annurev.nutr.27.061406.093734
49. Ruan H, Hacohen N, Golub TR et al (2002) Tumor necrosis factor-α suppresses adipocyte-specific genes and activates expression of preadipocyte genes in 3T3-L1 adipocytes: nuclear factor-κB activation by TNFis obligatory. Diabetes 51:1319–1336. https://doi.org/10.2337/diabetes.51.5.1319
50. Jin D, Sun J, Huang J et al (2014) TNF-α reduces g0s2 expression and stimulates lipolysis through PPAR-γ inhibition in 3T3-L1 adipocytes. Cytokine 69:196–205. https://doi.org/10.1016/j.cyto.2014.06.005
51. Kim JY, Tillison K, Lee J-H et al (2006) The adipose tissue triglyceride lipase ATGL/PNPLA2 is downregulated by insulin and TNFin 3T3-L1 adipocytes and is a target for transactivation by PPARγ. Am J Physiol Metab 291:E115–E127. https://doi.org/10.1152/ajpendo.00317.2005
52. Kaufmann RL, Matson CF, Rowberg AH, Beisel WR (1976) Defective lipid disposal mechanisms during bacterial infection in rhesus monkeys. Metabolism 25:615–624. https://doi.org/10.1016/0026-0495(76)90058-5
53. Kaufmann RL, Matson CF, Beisel WR (1976) Hypertriglyceridemia produced by endotoxin: role of impaired triglyceride disposal mechanisms. J Infect Dis 133:548–555. https://doi.org/10.1093/infdis/133.5.548
54. Feingold KR, Staprans I, Memon R et al (1992) Endotoxin rapidly induces changes in lipid metabolism that produce hypertriglyceridemia: low doses stimulate hepatic triglyceride production while high doses inhibit clearance. J Lipid Res 33:1765–1776
55. Lanza-jacoby S, Lansey SC, Cleary MP, Rosato FE (1982) Alterations in lipogenic enzymes and lipoprotein lipase activity during gram-negative sepsis in the rat. Arch Surg 117:144–147
56. Berg M, Fraker DL, Alexander HR (1994) Characterization of differentiation factor/leukaemia inhibitory factor effect of lipoprotein lipase activity and mRNA in 3T3-L1 adipocytes. Cytokine 6:425–432. https://doi.org/10.1016/1043-4666(94)90067-1
57. Li H, Chen X, Guan L et al (2013) MiRNA-181a regulates adipogenesis by targeting tumor necrosis factor-α (TNF-α) in the porcine model. PLoS One 8(10):e71568. https://doi.org/10.1371/journal.pone.0071568
58. Greenberg a S, Nordan RP, McIntosh J et al (1992) Interleukin 6 reduces lipoprotein lipase activity in adipose tissue of mice in vivo and in 3T3-L1 adipocytes: a possible role for interleukin 6 in cancer cachexia. Cancer Res 52:4113–4116
59. Lagathu C, Yvan-Charvet L, Bastard JP et al (2006) Long-term treatment with interleukin-1β induces insulin resistance in murine and human adipocytes. Diabetologia 49:2162–2173. https://doi.org/10.1007/s00125-006-0335-z
60. Oliveira A-C, Peixoto JR, de Arruda LB et al (2004) Expression of functional TLR4 confers proinflammatory responsiveness to *Trypanosoma cruzi* glycoinositolphospholipids and higher resistance to infection with *T. cruzi*. J Immunol 173:5688–5696. https://doi.org/10.4049/jimmunol.173.9.5688
61. Bafica A, Santiago HC, Goldszmid R et al (2006) Cutting edge: TLR9 and TLR2 signaling together account for MyD88-dependent control of parasitemia in *Trypanosoma cruzi* Infection. J Immunol 177:3515–3519. https://doi.org/10.4049/jimmunol.177.6.3515
62. Schaffler A, Scholmerich J (2010) Innate immunity and adipose tissue biology. Trends Immunol 31:228–235
63. Ajuwon KM, Banz W, Winters TA (2009) Stimulation with peptidoglycan induces interleukin 6 and TLR2 expression and a concomitant downregulation of expression of adiponectin receptors 1 and 2 in 3T3-L1 adipocytes. J Inflamm 6:8. https://doi.org/10.1186/1476-9255-6-8
64. Shi H, Kokoeva MV, Inouye K et al (2006) TLR4 links innate immunity and fatty acid-induced insulin resistance. J Clin Investig 116:3015–3025. https://doi.org/10.1172/JCI28898.TLRs
65. Kopp A, Buechler C, Neumeier M et al (2009) Innate immunity and adipocyte function: ligand-specific activation of multiple toll-like receptors modulates cytokine, adipokine, and chemokine secretion in adipocytes. Obesity 17:648–656. https://doi.org/10.1038/oby.2008.607
66. Schäffler A, Schölmerich J, Salzberger B (2007) Adipose tissue as an immunological organ: toll-like receptors, C1q/TNFs and CTRPs. Trends Immunol 28:393–399
67. Nagajyothi F, Desruisseaux MS, Thiruvur N et al (2008) *Trypanosoma cruzi* Infection of cultured adipocytes results in an inflammatory phenotype. Obesity 16:1992–1997. https://doi.org/10.1038/oby.2008.331
68. Hammarstedt A, Andersson CX, Rotter Sopasakis V, Smith U (2005) The effect of PPARgamma ligands on the adipose tissue in insulin resistance. Prostaglandins Leukot Essent Fatty Acids 73:65–75. https://doi.org/10.1016/j.plefa.2005.04.008

69. Odegaard JI, Ricardo-Gonzalez RR, Goforth MH et al (2007) Macrophage-specific PPARgamma controls alternative activation and improves insulin resistance. Nature 447:1116–1120. https://doi.org/10.1038/nature05894
70. Piccio L, Cantoni C, Henderson JG et al (2013) Lack of adiponectin leads to increased lymphocyte activation and increased disease severity in a mouse model of multiple sclerosis. Eur J Immunol 43:2089–2100. https://doi.org/10.1002/eji.201242836
71. Guo Q, Xu L, Liu J et al (2017) Fibroblast growth factor 21 reverses suppression of adiponectin expression via inhibiting endoplasmic reticulum stress in adipose tissue of obese mice. Exp Biol Med 242:441–447. https://doi.org/10.1177/1535370216677354
72. Martin H (2010) Role of PPAR-gamma in inflammation. Prospects for therapeutic intervention by food components. Mutat Res Fundam Mol Mech Mutagen 690:57–63
73. Rodrigues WF, Miguel CB, Chica JEL, Napimoga MH (2010) 15d-PGJ2 modulates acute immune responses to *Trypanosoma cruzi* infection. Mem Inst Oswaldo Cruz 105:137–143
74. Hovsepian E, Mirkin GA, Penas F et al (2011) Modulation of inflammatory response and parasitism by 15-deoxy-12,14 prostaglandin J2 in *Trypanosoma cruzi*-infected cardiomyocytes. Int J Parasitol 41:553–562. https://doi.org/10.1016/j.ijpara.2010.12.002
75. Penas F, Mirkin GA, Hovsepian E et al (2013) PPARγ ligand treatment inhibits cardiac inflammatory mediators induced by infection with different lethality strains of *Trypanosoma cruzi*. Biochim Biophys Acta Mol Basis Dis 1832:239–248. https://doi.org/10.1016/j.bbadis.2012.08.007
76. Liu LF, Purushotham A, Wendel A et al (2009) Regulation of adipose triglyceride lipase by rosiglitazone. Diabetes Obes Metab 11:131–142. https://doi.org/10.1111/j.1463-1326.2008.00916.x
77. Festuccia WT, Blanchard P-G, Turcotte V et al (2009) Depot-specific effects of the PPARgamma agonist rosiglitazone on adipose tissue glucose uptake and metabolism. J Lipid Res 50:1185–1194. https://doi.org/10.1194/jlr.M800620-JLR200
78. Watkins SM, Reifsnyder PR, Pan H et al (2002) Lipid metabolome-wide effects of the PPARγ agonist rosiglitazone. J Lipid Res 43:1809–1817. https://doi.org/10.1194/jlr.M200169-JLR200
79. Martin G, Schoonjans K, Staels B, Auwerx J (1998) Pparγ activators improve glucose homeostasis by stimulating fatty acid uptake in the adipocytes. Atherosclerosis 137(Suppl):S75–S80
80. Kersten S (2001) Mechanisms of nutritional and hormonal regulation of lipogenesis. EMBO Rep 2:282–286